Jinst
Published by IOP Publishing for Sissa Medialab
Received: *March 16, 2026*
Accepted: *April 13, 2026*
Published: *April 30, 2026*

7th International Workshop on New Photon-Detector
Bologna, Italy
3–5 December 2025

The focal plane cameras of the ASTRI Mini-Array air-Cherenkov telescopes for gamma ray astronomy

G. Sottile,[a,*] P. Sangiorgi,[a] C. Gargano,[a] F. Lo Gerfo,[a] M. Corpora,[a] D. Mollica,[a] G. Contino,[a] T. Mineo,[a] O. Catalano,[a] M. Capalbi,[b] G. Leto,[c] A. Micciché,[c] G. Bellassai,[c] M. Bellassai,[c] E. Martinetti,[c] G. Nicotra,[c] C. Lauretta,[c] S. Scuderi,[d] A. Crestan,[d] A. Giuliani,[d] M. Buzzi,[e] G. Pareschi,[e] L. Lessio,[f] G. Tosti,[g] A. Abba,[h] F. Caponio,[h] A. Cusimano,[h] J. Fluery,[i] S. Ahmad,[i] J.B. Cizel[i] and F. Perez[i]

[a]*INAF IASF-Pa, Palermo, Italy*
[b]*INAF OAR, Roma, Italy*
[c]*INAF OACT, Catania, Italy*
[d]*INAF IASF-Mi, Milano, Italy*
[e]*INAF OABrera, Milano, Italy*
[f]*INAF OAPD, Padova, Italy*
[g]*Università degli Studi di Perugia, Perugia, Italy*
[h]*Nuclear Instruments, Lambrugo (CO), Italy*
[i]*Weeroc, Villebon-sur Yvette, France*

E-mail: giuseppe.sottile@inaf.it

Abstract: This work describes the design, development, and calibration of cameras for the nine innovative dual-mirror imaging atmospheric Cherenkov telescopes of the ASTRI Mini-Array project. This international initiative, led by the Italian National Institute for Astrophysics (INAF), focuses on ground-based gamma-ray astronomy using the air Cherenkov technique. Located at the Observatorio del Teide in Tenerife, Canary Islands, the ASTRI Mini-Array will perform high-sensitivity, high-angular-resolution observations of the gamma-ray universe across the 1 TeV to a few hundred TeV energy range. The cameras used in the ASTRI Mini-Array are the ultimate evolution of the prototype system tested at the ASTRI-Horn telescope pathfinder since 2016 [1], on the slopes of Mount Etna in Sicily, Italy. This prototype provided valuable experience with gamma-ray observations using the atmospheric Cherenkov technique, dual-mirror optics, and cameras based on multi-pixel Silicon Photo Multiplier (SiPM) detectors. The new ASTRI cameras incorporate SiPM technology, using

*Corresponding author.

https://doi.org/10.1088/1748-0221/21/04/C04090

2026 JINST 21 C04090

fast, low-power peak detectors thanks to the custom ASIC CITIROC, developed jointly by INAF and the French company Weeroc. Since the initial design phases, the camera has incorporated advanced, efficient engineering solutions to enhance its performance and effectiveness. Built into the structure, the thermal control system (which requires no external cooling liquids) and the focal plane calibration subsystems ensure operational efficiency, reliability, and ease of installation — crucial for maintaining a fully operational array with multiple telescopes. The first Cherenkov camera was installed on the first (ASTRI-1) telescope in late August 2024, while the installation of the remaining cameras is ongoing. This paper discusses the layout and subsystems of the camera design and presents performance results from calibrating the first installed camera.

Keywords: Cherenkov detectors; Gamma telescopes; Solid state detectors; Front-end electronics for detector readout

2026 JINST 21 C04090

Contents

1 Introduction

The ASTRI Mini-Array is an innovative project led by INAF, designed to conduct high-sensitivity observations of the very-high-energy gamma-ray sky in the 1–200 TeV energy range [2, 3]. Its telescopes feature dual-mirror Schwarzschild-Couder optics [4, 5], and a compact Cherenkov camera based on Silicon Photomultipliers (SiPMs), as shown in figure 1. The camera is built to provide a wide field of view along with excellent spatial and temporal resolution.

This paper provides a detailed overview of the ASTRI camera, focusing on its key subsystems, including the focal plane, front-end and back-end electronics, voltage distribution board, thermal control, calibration system, and control software. It also reports the first-year scientific performance of ASTRI-1, highlighting observations of the Crab Nebula [6] and the successful detection of the first stereoscopic Cherenkov event with ASTRI-1 and ASTRI-3. Additionally, the paper reviews the current status of camera deployment and discusses future developments.

2 Camera subsystems

The ASTRI Mini-Array camera architecture features a modular design, with dedicated subsystems managing photon detection, signal processing, triggering, power distribution, thermal stabilization, and calibration [7]. These subsystems work together to maintain stable performance across a variety of observational conditions. The following sections explain the main camera subsystems in detail.

Figure 1. Left: ASTRI Mini-Array camera. Right: ASTRI 1 telescope.

2026 JINST 21 C04090

2.1 Focal plane

The Cherenkov camera designed for the ASTRI Mini-Array uses SiPMs. The focal plane includes 37 Photon Detection Modules (PDMs), each made up of three main boards: the SiPM board, the ASIC board, and the FPGA board, see figure 2.

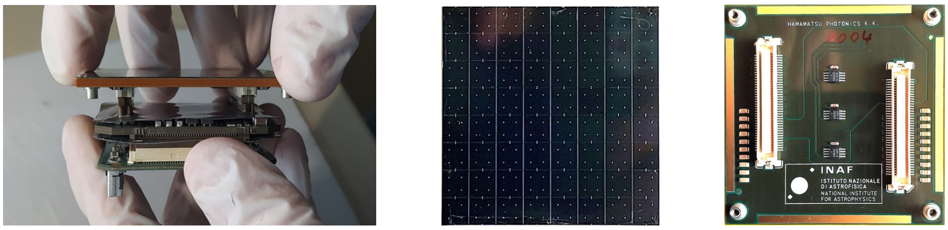

Figure 2. Left: PDM. Center: top view of the SiPM tile. Right: bottom view of the SiPM tile showing the location of the temperature sensors.

Each SiPM board contains 64 pixels, each measuring 7 mm × 7 mm, see figure 2. This is the largest pixel size used in SiPM-based cameras for imaging atmospheric Cherenkov telescopes so far. The photodetectors are positioned at the telescope's focal plane and collectively define the camera's spherical focal surface (according to the Schwarzschild-Couder configuration). The entire focal plane, see figure 3, includes 2368 pixels, offering a field of view (FoV) of 10.5°, the broadest achieved for this type of telescope.

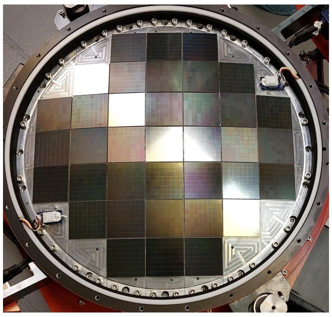

Figure 3. The complete focal plane of the ASTRI Mini-Array camera, populated with 37 Photon Detection Modules for a total of 2368 SiPM pixels.

The adopted photodetectors are Hamamatsu S14521 SiPMs, featuring 75 µm microcells, a photon detection efficiency (PDE) ranging from 50% to 54% in the 405–459 nm wavelength interval, and an average dark count rate (DCR), measured at 0.5 photoelectron (PE) and 15°C, of approximately 2.8×10^6 counts per second. At INAF's request, the devices were delivered without any protective optical coating. Although this choice increases the complexity of the assembly process, it reduces optical crosstalk to as low as 4.5%.

Three temperature sensors are installed on the bottom side of each SiPM board, see figure 2. These sensors continuously monitor the detectors' temperature and enable dynamic adjustment of the bias voltage to ensure stable gain over time. Although the SiPMs and the temperature sensors are separated by the FR4 layer of the printed circuit board, the layout has been optimized to minimize thermal resistance. Furthermore, a dedicated calibration procedure correlating the sensor readings with the actual SiPM temperature ensures that the residual measurement uncertainty is negligible.

2026 JINST 21 C04090

The ASTRI Mini-Array camera is designed to operate under high night-sky background (NSB) conditions, thereby increasing the observing duty cycle compared to the ASTRI-Horn camera [8, 9]. Under such conditions, the SiPMs experience higher currents, leading to increased heat generation in temperature-sensitive devices. Therefore, the thermal design of the tile support structure is essential, as it ensures rapid heat removal and maintains low, uniform operating temperatures. The support structure has been specifically designed to balance the temperature distribution across each tile and to dissipate power levels of up to 3.15 W per tile.

2.2 Front-end electronics

The Front-End Electronics (FEE) of the ASTRI camera uses the CITIROC Application-Specific Integrated Circuit (ASIC), developed by Weeroc together with INAF, as an evolution of the EASIROC chip. CITIROC is specifically designed for SiPM readout and is one of the main features that distinguish the ASTRI camera from other high-energy Cherenkov cameras.

Each CITIROC offers 32 channels for signal processing; therefore, two chips are used to read out the 64 pixels of a single PDM, see figure 4. Each channel has a dynamic range from 0 to 2000 PE (for a SiPM gain of 10^6), achieved through two parallel preamplifier chains (High Gain – HG — and Low Gain – LG). This dual-gain architecture ensures a wide dynamic range without requiring an additional external preamplifier stage, thereby maintaining a high signal-to-noise ratio.

Within the CITIROC, the SiPM signal is simultaneously routed to the high- and low-gain amplitude chains and a dedicated timing chain. After the preamplifier stage, the signal is processed by a programmable slow shaper, whose output feeds a peak detector circuit. The peak detector stage was introduced by Weeroc at the specific request of INAF, allowing for the direct extraction of the signal maximum without waveform sampling. The camera digitizes and transfers only the peak values associated with triggered events to the remote camera server. This architecture significantly reduces the amount of scientific data generated compared to high-sampling-rate waveform acquisition systems, while avoiding real-time data skimming algorithms that are typically power demanding.

The 32 trigger signals are generated by comparing the outputs of the fast shapers with a common threshold supplied by a 10-bit DAC. The stored HG and LG peak values are sequentially multiplexed and digitized by two dedicated 14-bit ADCs for each CITIROC.

The two CITIROCs, the ADCs, and the ancillary electronics hosted on the ASIC board are connected to a Xilinx Artix-7 FPGA on the FPGA board, see figure 4. This FPGA controls the ASIC configuration tables and executes the programmable topological trigger algorithm.

The topological trigger block produces a PDM trigger when signals from neighboring pixels surpass the programmable threshold within a set time window. This setup is crucial for preventing false triggers, such as when a bright star moves into the view and lights up multiple pixels. By filtering out unwanted triggers, the system improves the detection of Cherenkov events and boosts telescope performance. During normal operation of the ASTRI Mini-Array camera, the topological trigger condition is usually configured to detect at least 4 contiguous pixels within a coincidence window of a few nanoseconds. The PDM trigger signal is then sent to the Back-End Electronics (BEE) to initiate the Camera Trigger.

The FPGA on the front-end board also calculates real-time variance for each of the 64 pixels in the tile. Originally introduced to estimate the NSB level [10] even with the CITIROC's AC-coupled inputs, this variance tool has become a key diagnostic instrument. It provides immediate feedback on

2026 JINST 21 C04090

the focal plane's health status during pre-observation phases and helps verify telescope pointing [11]. The variance calculation adds no acquisition dead time, as it is performed during the intervals between consecutive trigger events.

In addition, the FPGA timestamps the 64 pixel-level trigger signals relative to the PDM trigger event. This functionality, implemented in the ASTRI Mini-Array camera, allows reconstruction of the temporal sequence of triggered pixels and, consequently, determination of the direction of event propagation across the focal plane.

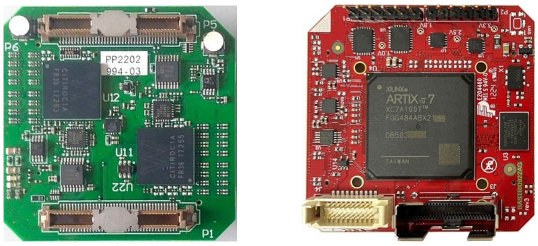

Figure 4. Left: ASIC board with two CITIROCs. Right: FPGA board.

2.3 Back-end electronics

The Back-End Electronics (BEE) (see figure 5) connects all camera subsystems and manages communication with external servers. Its architecture is built around a Xilinx Zynq-7000 SoC running a Linux operating system, complemented by two additional Xilinx Artix-7 FPGAs.

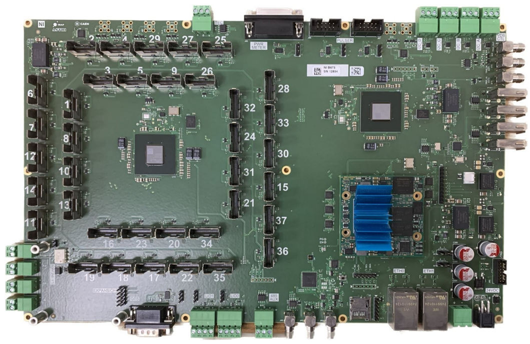

Figure 5. Back-End Electronics board of the ASTRI Mini-Array camera.

The first Artix-7 FPGA is dedicated to generating camera triggers. It monitors the 37 differential PDM trigger lines and, upon detecting a valid PDM trigger, outputs the camera trigger signal, which is then sent back to all PDMs to start event acquisition.

The second Artix-7 handles communication between the Zynq device and the 37 PDMs via Serial Peripheral Interface (SPI) and UART links. Scientific event data and variance data are received through SPI connections, while configuration tables for the CITIROCs and PDM FPGAs are sent from the BEE. Housekeeping data is collected through 37 separate UART interfaces.

All incoming data is formatted according to the specified protocol and transmitted to the nearby camera server via TCP/IP. The BEE also manages the 10 MHz reference clock and the Pulse-Per-Second (PPS) signals supplied by the White Rabbit system, enabling sub-nanosecond synchronization

2026 JINST 21 C04090

across the telescopes in the array. The distributed reference clock and PPS signals are used to accurately timestamp triggered events.

2.4 Voltage distribution board

The Voltage Distribution Board (VDB) supplies power to the PDMs. It has a modular design where each PDM is connected to a dedicated VDB-PDM module. The BEE communicates with all VDB-PDM modules through four separate I^2C buses.

Each VDB-PDM supplies the necessary low-voltage rails for the PDM electronics and the high voltage for SiPM biasing. The high-voltage module can provide currents up to 70 mA in the 35–45 V range, allowing stable operation during bright night-sky conditions and thereby increasing the observing duty cycle. Maximizing the duty cycle is a key requirement for imaging atmospheric Cherenkov telescopes and is especially important for Small-Sized Telescopes working at the highest energies, where photon statistics are naturally limited.

2.5 Thermal control system

Silicon Photomultipliers show a strong temperature dependence, especially in gain and dark current. The ASTRI Mini-Array camera is the only SST-class camera equipped with a fully integrated thermal control system using Peltier thermoelectric coolers (TECs). This design keeps the SiPM temperature stable without liquid cooling systems or external chillers, making installation and maintenance simpler.

The system keeps the photodetectors' temperature within ±1 °C across the entire focal plane for ambient temperatures in the range −10 °C to +25 °C, under continuous illumination corresponding to 70 mA per tile.

Twelve Peltier cells mounted on the underside of the Focal Plane Support Structure remove heat produced by the FEEs and SiPMs through a low-thermal-resistance path that includes aluminum structures and high-performance thermal interface materials. The excellent performance of the thermal control system greatly enhances pre-operation procedures for nighttime observations. The focal plane reaches its target operating temperature within just a few minutes.

For example, starting from an ambient temperature of 23 °C at sea level, the focal plane stabilizes at 15 °C (±1 °C) in about 11 minutes. Tests performed at ambient temperatures between 23 °C and 25 °C consistently confirm the durability and repeatability of this performance.

2.6 Calibration system

The ASTRI Mini-Array camera is equipped with an embedded calibration system that performs relative calibration [12] of the focal plane and acquisition chain. The system is engineered to operate also during the daytime in order to maximize the observing duty cycle. A dedicated lid and sealing system ensures complete light-tightness; with the lids closed, ambient light is kept from reaching the photodetectors through a light-tight system traps.

Under these controlled conditions, calibration procedures such as breakdown-voltage measurements, staircase-curve acquisitions, and pulse-height distribution (PHD) measurements can be performed. All calibration activities are conducted with the focal plane in thermal equilibrium.

The breakdown-voltage procedure determines the optimal high-voltage bias for each pixel under weak, continuous illumination. PHD curves, acquired using 10 ns laser light pulses, allow evaluation

2026 JINST 21 C04090

of the single PE in terms of ADC digital counts for each pixel. Staircase curves, measured in dark conditions, provide the PE scale in 10-bit DAC threshold units.

The system's hardware includes blue and green laser diodes connected to a side-glow optical fiber that runs along the edge of the camera's entrance window. The light emitted sideways by the fiber couples with the window glass and, through controlled scattering, evenly illuminates all PDMs on the focal plane.

3 Camera control software

The camera features dedicated control software operating on the Processing Unit of the BEE. This software handles all hardware subsystems and facilitates slow control operations.

The architecture is modular and composed of several independent software components that operate as background services (daemons). Each module handles a specific subsystem, gathering housekeeping data and performing the relevant control actions. All monitored parameters and camera functions are accessible through an Open Platform Communications Unified Architecture (OPC UA) server, which offers a standardized interface for remote access.

This interface enables remote operation of the camera via various software clients designed for specific purposes and operational contexts. These include the Cherenkov Camera Software Supervisor [13] of the ASTRI Mini-Array Supervisory Control and Data Acquisition (SCADA) [14] system, used for high-level control during standard array operations, as well as the AIV/AIT software client employed during the Assembly, Integration, and Testing phases of the instrument.

The control software has been developed internally at INAF and is supported by a specialized engineering GUI. This tool is used to test all camera subsystems, quickly visualize monitored and acquired data, and run specific data acquisition procedures for calibration.

4 First-year scientific results

During its first year of scientific operations (2024–2025), ASTRI-1 gathered over 250 hours of observations across 43 nights, covering both standard and high-zenith configurations as well as off-axis pointings up to 3.5° [15]. The Crab Nebula served as the primary calibration and benchmark source.

With 9 hours of exposure, a detection significance of approximately 10 sigma was achieved, and the energy spectrum was reconstructed up to roughly 20 TeV, consistent with measurements from other Imaging Atmospheric Cherenkov Telescopes (IACTs). The reconstructed source location is within 0.03 degrees of the nominal Crab coordinates.

Event rates during dark observations ranged between 80–95 Hz and between 50–60 Hz under moonlight. Stable operation was demonstrated up to 70% lunar phase, corresponding to a Crab detection rate of 14.6 ± 2.1 events per hour and an effective annual observing time of approximately 1900 hours.

Off-axis measurements indicate a flat acceptance up to 2.5°, with a $\sim 40\%$ decrease at 3.5°. The achieved performance includes a sensitivity of ~ 0.25 Crab at 2 TeV, an energy threshold of ~ 1 TeV, an angular resolution between 0.15° and 0.3°, an energy resolution of 20–25%, and an energy bias below 10%. Moreover, the first stereoscopic Cherenkov event was successfully recorded by ASTRI-1 and ASTRI-3 immediately after the installation of the latter (see figure 6).

2026 JINST 21 C04090

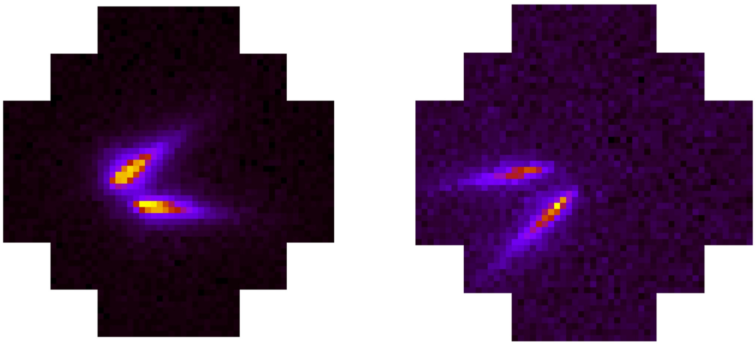

Figure 6. The first two stereoscopic Cherenkov events detected by the ASTRI 1 and ASTRI 3 telescopes in November 2025.

5 Conclusions

The ASTRI camera design features elegant, robust, and highly innovative engineering solutions, including 7 mm SiPM pixels that provide excellent spatial resolution, a large 10.5° field of view for extensive sky coverage, a low-noise, low-power, high-performance peak detector, a fully integrated and self-contained thermal control system, reliable operation even under strong night-sky background conditions, and a calibration system capable of functioning during daylight, thus maximizing nighttime observation time.

During its first year of scientific operations, ASTRI-1 achieved high-significance detections of the Crab Nebula, accurate energy and position reconstruction, stable operation under both dark and moonlit conditions, and recorded the first stereoscopic Cherenkov event with ASTRI-1 and ASTRI-3, confirming the system's readiness for coordinated array observations.

Looking ahead, at least three more cameras will be installed by summer 2026, and the complete set of nine telescopes will be operational by the end of 2026. This will finalize the expansion of the ASTRI Mini-Array and enable high-sensitivity, wide-field observations of the very-high-energy gamma-ray sky.

Acknowledgments

This work was conducted in the context of the ASTRI Project. We gratefully acknowledge support of the people, agencies, and organizations listed here: `http://www.astri.inaf.it/en/library/`.

We are grateful to all the companies that supported the development and realization of the ASTRI cameras and, in particular, CAEN, EIE GROUP, Hamamatsu Photonics, Nuclear Instruments, Umas Technology, Weeroc and Zaot.

References

[1] G. Pareschi, *The ASTRI SST-2M prototype and mini-array for the Cherenkov Telescope Array (CTA)*, *Proc. SPIE* **9906** (2016) 99065T.

[2] S. Vercellone et al., *ASTRI Mini-Array core science at the Observatorio del Teide*, *JHEAp* **35** (2022) 1 [`arXiv:2208.03177`].

[3] S. Scuderi et al., *The ASTRI Mini-Array of Cherenkov telescopes at the Observatorio del Teide*, *JHEAp* **35** (2022) 52 [`arXiv:2208.04571`].

[4] G. Sironi, *Aplanatic telescopes based on Schwarzschild optical configuration: from grazing incidence Wolter-like x-ray optics to Cherenkov two-mirror normal incidence telescopes*, *Proc. SPIE* **10399** (2017) 1039903.

[5] E. Giro et al., *Tests characterization and alignment for the optics of the ASTRI SST-2M telescope prototype for the Cherenkov Telescope Array*, *Proc. SPIE* **9151** (2014) 91513L.

[6] S. Lombardi et al., *First detection of the Crab Nebula at TeV energies with a Cherenkov telescope in a dual-mirror Schwarzschild-Couder configuration: the ASTRI-Horn telescope*, *Astron. Astrophys.* **634** (2020) A22 [arXiv:1909.12149].

[7] G. Sottile et al., *The ASTRI Cherenkov Camera: from the Prototype to the Industrial Version for the Mini-Array*, in the proceedings of the *2022 IEEE Nuclear Science Symposium (NSS)*, Italy (2022), p. 1–5 [DOI:10.1109/NSS/MIC44845.2022.10399133] [arXiv:2301.09915].

[8] O. Catalano et al., *The ASTRI SST-2M Prototype: Camera and Electronics*, in the proceedings of the *33rd International Cosmic Ray Conference*, Rio de Janeiro, Brazil, 2–9 July 2013 [arXiv:1307.5142].

[9] G. Sottile et al., *ASTRI SST-2M camera electronics*, *Proc. SPIE* **9906** (2016) 99063D.

[10] A. Segreto et al., *Calibration and monitoring of the ASTRI-Horn telescope by using the night-sky background measured by the photon-statistics ("variance") method*, *PoS* **ICRC2019** (2020) 791 [arXiv:1909.08750].

[11] S. Iovenitti et al., *Assessment of the Cherenkov camera alignment through Variance images for the ASTRI telescope*, *Exper. Astron.* **53** (2022) 117 [arXiv:2111.02745].

[12] D. Mollica et al., *Calibration procedures for the ASTRI Mini-Array Cherenkov cameras*, *J. Phys. Conf. Ser.* **3053** (2025) 012036.

[13] M. Corpora et al., *Design and development of the Supervisor software component for the ASTRI Mini-Array Cherenkov Camera*, *Proc. SPIE* **12189** (2022) 121891Z.

[14] ASTRI collaboration, *Software architecture and development approach for the ASTRI Mini-Array project at the Teide Observatory*, *J. Astron. Telesc. Instrum. Syst.* **10** (2024) 017001.

[15] S. Crestan et al., *ASTRI-1: Early Data and Performance Highlights*, *PoS* **ICRC2025** (2025) 617.